J Fluoresc (2010) 20:599–606
DOI 10.1007/s10895-009-0593-5

ORIGINAL PAPER

Fluorescence Lymph Node Mapping in Living Mice Using Quantum Dots and a Compression Technique

Yusuke Inoue · Shigeru Kiryu · Makoto Watanabe · Naoki Oyaizu · Kuni Ohtomo

Received: 27 August 2009 / Accepted: 30 December 2009 / Published online: 16 January 2010

Abstract The lymphatic system is essential in oncology and immunology, and in vivo fluorescence imaging plays a major role in assessing the lymphatic drainage. We investigated non–invasive fluorescence lymph node mapping in mice with special reference to the assessment of deep abdominal lymph nodes. Quantum dots were injected subcutaneously into the rear footpads of mice, and the time course of the fluorescent signal was assessed. Visualization of abdominal lymph nodes was compared with and without compression of the abdomen with transparent, colorless tape at injection doses of 1, 5, and 20 pmol. Popliteal, sacral, iliac, and renal lymph nodes were delineated by non–invasive imaging. Lymph node signals increased up to 3 h after injection. Compression of the abdomen markedly improved the visualization of the iliac nodes, which were invisible at 5 pmol without compression and visible at 1 pmol with compression. Fluorescence lymph node mapping using quantum dots allowed the visualization of deep abdominal lymph nodes in addition to superficial nodes in intact mice, with the aid of a simple compression technique.

Y. Inoue (✉) · S. Kiryu · M. Watanabe
Department of Radiology, Institute of Medical Science,
University of Tokyo,
4-6-1 Shirokanedai,
Minato-ku, Tokyo 108-8639, Japan
e-mail: inoueys-tky@umin.ac.jp

N. Oyaizu
Department of Laboratory Medicine, Institute of Medical Science,
University of Tokyo,
Tokyo, Japan

K. Ohtomo
Department of Radiology, Graduate School of Medicine,
University of Tokyo,
Tokyo, Japan

Keywords Fluorescence imaging · Quantum dots · Lymph node · Near-infrared fluorescence · Mouse

Introduction

Semiconductor quantum dots (QDs) are bright, stable fluorophores with favorable properties, including size- and composition-tunable fluorescence emission, narrow and symmetric emission spectra, and broad excitation spectra [1–3] and used for in vivo imaging. QDs are taken up by the lymph nodes and retained for a long time after subcutaneous injection. They can be used for sentinel lymph node mapping in animal experiments [4–7] and have potential applications in human clinical practice. Light in the 600–900-nm wavelength range can travel relatively long distances in vivo [8], and thus QDs emitting far-red or near-infrared (NIR) light are preferred for in vivo imaging, including fluorescence lymph node mapping. However, scattering and absorption of light is still a major limitation in optical imaging in the far-red or NIR regions, causing attenuation and diffusion of light signals. Most fluorescence imaging studies employ fluorescence reflectance imaging, in which the application of excitation light and detection of emission light are performed on the same side of the animal. The effects of absorption and scattering are much more severe for deep sources than for superficial sources in fluorescence reflectance imaging because of the longer light path [9]. Therefore, although fluorescence lymph node mapping can clearly visualize superficial lymph nodes in intact animals, it is difficult to obtain high-quality images of deeply located lymph nodes.

Although knowledge about the lymphatic system should be essential in immunology and oncology, the lymphatic drainage pattern has not been fully established in mice. The

investigation of the murine lymph nodes appears to be disturbed by their small sizes and may be significantly aided by in vivo imaging. In this study, we performed lymph node mapping in intact living mice after the subcutaneous injection of NIR QDs using fluorescence reflectance imaging. In an attempt to enhance the visualization of deep abdominal lymph nodes, we decreased the thickness of the abdomen using a simple compression technique. The principal aim of our study was to evaluate fluorescence lymph node mapping in the non-invasive visualization of deep abdominal lymph nodes.

Materials and methods

Animals

Female BALB/c mice (10–14 weeks old) were used for the experiments. They were obtained from SLC Japan (Hamamatsu, Japan) and were handled according to the guidelines of the Institute of Medical Science, University of Tokyo. Mice were maintained on a regular rodent diet (CA-1; CLEA Japan, Tokyo, Japan) until switching to a purified diet described below. Hair was removed with depilatory mousse (Epilat, Kracie, Tokyo, Japan) prior to imaging. The experiments were approved by the committee for animal research at our institution.

CCD camera

All imaging studies were performed using a cooled charge-coupled device (CCD) camera system (IVIS Imaging System 100; Xenogen, Alameda, CA), equipped with a fluorescence kit (XFO-6; Xenogen). Data were acquired in the far-red and NIR regions. Excitation and emission filters with passbands of 615–665 nm and 695–770 nm (Xenogen), respectively, were used for far-red imaging, and excitation and emission filters with passbands of 672.5–747.5 nm and 775–825 nm (Chroma Technology, Rockingham, VT), respectively, were used for NIR imaging. For image acquisition, mice were anesthetized by isoflurane inhalation and placed in the light-tight chamber of the CCD camera system. The signal intensity was quantified using the Living Image software (version 2.50; Xenogen).

Diet and autofluorescence

Autofluorescence in the gastrointestinal system was assessed serially after the substitution of a purified diet (Diet No. A10000, CLEA Japan) for the regular diet. On day 0, ventral fluorescence images in the far-red and NIR regions were acquired from 12 mice fed the regular diet, with no administration of fluorescent agents. Three mice were imaged simultaneously. The field of view (FOV) was 25 cm and binning was 4. The exposure time was 1 s for far-red imaging and 10 s for NIR imaging. High- or low-intensity excitation light can be selected in the imaging system; high-intensity light was used in this experiment. After the completion of day-0 imaging, the mice were moved to new cages and fed a purified diet, and imaging was repeated 1, 2, 4, and 7 days later. Six mice were housed in cages with wire racks placed at their bottoms to prevent the intake of feces, and six mice were housed in cages without wire racks. A region of interest (ROI) of a fixed size was set in the abdomen, and the mean signal intensity ($p/s/cm^2/sr$) in the ROI was determined.

Fluorescence lymph node mapping

To reduce gastrointestinal autofluorescence, mice were fed the purified diet instead of the regular diet for at least 2 days before fluorescence lymph node mapping. During the dietary preparation, mice were housed in cages with wire racks placed at their bottoms. For fluorescence lymph node mapping, mice were subcutaneously injected with Qdot 800 ITK Carboxyl Quantum Dots (carboxyl QDs; Invitrogen, Grand Island, NY) in the dorsal side of the right rear footpad, using a microsyringe. The emission peak of the QDs was 800 nm. The injection dose was 1, 5, or 20 pmol per mouse. The QD solution was diluted with phosphate-buffered saline, and the volume injected was fixed at 10 μL. A gentle massage was applied to the injection site for about 15 s immediately after injection.

After QD injection, ventral fluorescence images were acquired under up to four different conditions. A ventral image was acquired with the posterior limbs fixed with colorless, transparent tape. The dorsal sides of the rear footpads faced the camera to assess residual fluorescence at the injection site. Subsequently, ventral images were acquired after shielding the right rear foot (foot shielding) and then after shielding the right rear foot and right popliteal lymph node (foot and knee shielding). For shielding, the area of intense fluorescence was covered with black, opaque tape. Moreover, the abdomen was compressed towards the imaging table with colorless, transparent tape to reduce the thickness of the abdomen and enhance the visualization of deep structures (Fig. 1). In compression imaging, shielding of the right rear foot and right popliteal lymph node was also performed. Additionally, dorsal fluorescence images were acquired under up to three different conditions. First, a dorsal image was obtained after shielding the right rear foot (foot shielding) and then after shielding the right rear foot, right popliteal lymph node, and right sacral lymph node (foot and hip shielding). Finally, a compression image was obtained with the abdomen compressed towards the imaging table. For

Fig. 1 Compression of the abdomen of a mouse with colorless, transparent tape. The mouse was placed in the supine position. The right rear foot and right knee were shielded with black tape

comparison, three baseline images, two ventral images with and without compression and one dorsal image without compression, were obtained before QD injection. No shielding was used in baseline imaging. In fluorescence lymph node mapping, one mouse was imaged at a time in the NIR region. The FOV was 20 cm and binning was 2. The exposure time and intensity of excitation light are specified in the following sections.

Time course after QD injection

We assessed the time course of light signals in fluorescence lymph node mapping. Three mice were injected with 20 pmol carboxyl QDs in the right rear footpad. In vivo fluorescence imaging was performed before and 10 min after injection, followed by imaging at 1, 3, and 24 h after injection. At 10 min, ventral images without shielding and with foot shielding and a dorsal image with foot shielding were acquired. The images obtained at 1, 3, and 24 h included four ventral images (without shielding, with foot shielding, with foot and knee shielding, and with compression) and a dorsal image with foot shielding. The exposure time was 1 s in imaging without shielding after QD injection and 10 s otherwise. Low-intensity light was used for excitation.

After the completion of 24-h imaging, ex vivo fluorescence imaging was performed. Mice were sacrificed and the tissues corresponding to focal signals indicative of lymph node accumulation were excised. The excised tissues and the remaining body were imaged with the CCD camera to confirm that the excised tissues were the sources of the focal signals.

ROIs were placed for the right rear footpad, right popliteal lymph node, right sacral lymph node, iliac lymph node, and renal lymph node, and the mean signal in each ROI (p/s/cm^2/sr) was determined. ROIs of the same size were used for a given area. An ROI for the footpad was placed on the ventral image without shielding. ROIs for the popliteal, sacral, and renal nodes were drawn on the dorsal image. When the lymph node was not visualized, an ROI was set at the presumed location. An ROI for the iliac node was drawn on the ventral compression image. The signal for the iliac node was not assessed 10 min after injection because compression imaging was not performed at this time point.

Techniques to enhance visualization of lymph nodes

We evaluated the effect of shielding and compression on the visualization of lymph nodes. After baseline imaging, five mice were injected with 20 pmol carboxyl QDs in the right rear footpad, and fluorescence lymph node mapping was performed 3 h later. Four ventral images were collected: without shielding, with foot shielding, with foot and knee shielding, and with compression. Three dorsal images were also acquired: with foot shielding, with foot and hip shielding, and with compression. The exposure time was 20 s before QD injection, 2 s for ventral imaging after QD injection, and 5 s for dorsal imaging after QD injection. High-intensity light was used for excitation.

ROIs were placed for the iliac lymph node on the ventral images with foot and knee shielding and with compression, and the maximum signals in the ROIs were determined. ROIs of a fixed size were taken in the left flank as a background region for the images, and the mean signals were computed. The ratio of the maximum signal for the iliac lymph node to the mean signal for the background region was calculated for each image to define the iliac lymph node/background contrast. The contrast with compression was divided by that without compression, and the enhancement ratio was determined. Similarly, the effect of compression was assessed for the renal lymph node. ROIs were placed for the renal lymph node and left flank on the dorsal images with foot and hip shielding and with compression, and the renal lymph node/background contrast and the enhancement ratio were determined.

Reduction of injection dose

We also evaluated the visualization of lymph nodes at lower injection doses. Three and four mice were injected with 5 and 1 pmol carboxyl QDs in the right rear footpad, respectively, and fluorescence lymph node mapping was performed 3 h later. Four ventral images were collected: without shielding, with foot shielding, with foot and knee

shielding, and with compression. Three dorsal images were acquired: with foot shielding, with foot and hip shielding, and with compression. The exposure time was 8 s for ventral imaging after the injection of 5 pmol QDs and 20 s otherwise. High-intensity excitation light was used.

Results

Diet and autofluorescence

Strong gastrointestinal autofluorescence was observed in the far-red and NIR regions for mice fed a regular diet. Autofluorescence decreased dramatically on day 1, 1 day after substitution of a purified diet for the regular diet (Fig. 2), and a further slight reduction was observed in some mice on day 2. Conspicuous gastrointestinal signals were no longer observed on day 2, and thereafter essentially no change in autofluorescence intensity was demonstrated. The time course and intensity of autofluorescence were not influenced by the use of a wire rack placed at the bottom of the cage.

Time course after QD injection

After the injection of 20 pmol carboxyl QDs into the rear footpad, in vivo fluorescence lymph node mapping demonstrated focal signals indicative of accumulation in the popliteal, sacral, iliac, and renal lymph nodes. Ventral images showed the popliteal and iliac nodes, and dorsal images showed the popliteal, sacral, and renal nodes. Ex vivo fluorescence imaging indicated that the focal signals were due to QD uptake in the presumed lymph nodes. The presumed iliac lymph nodes from three mice and renal lymph nodes from two mice were examined histologically using hematoxylin eosin staining and were confirmed to be lymph node tissues.

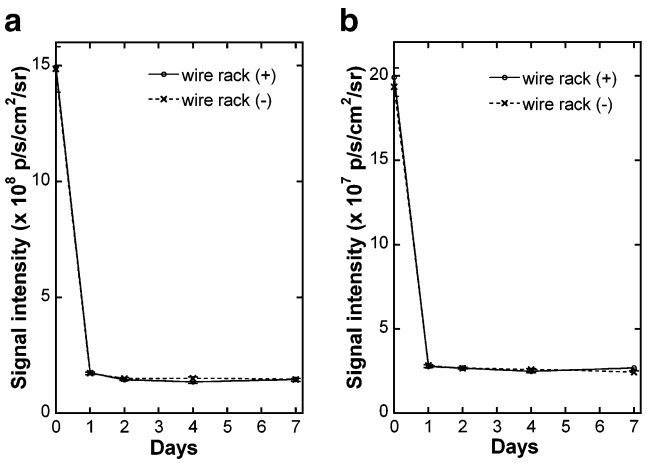

Fig. 2 Time course of mean autofluorescence in the far-red **a** and NIR regions **b**. All mice were fed a purified diet instead of the regular diet after day-0 imaging. The solid and broken lines represent abdominal fluorescence with and without the wire rack at the bottom of the mouse cage, respectively. Error bars show standard errors (n=6)

Fluorescence at the injection site decreased gradually during the 24–h examination period (Fig. 3a). Fluorescence in the lymph nodes increased up to 3 h after injection and was similar between 3- and 24–h imaging (Fig. 3b). At 10 min, the popliteal and sacral lymph nodes, together with their afferent pathways, were visualized. Compression images were not obtained, and the iliac nodes were not observed. At 1 h, although the iliac nodes were not detected in two of the three mice without compression, they were clearly observable in compression images. In the other mouse, the iliac node was apparent without compression, but compression greatly enhanced visualization. At 3 and 24 h, the iliac nodes were visualized in three mice without compression and more clearly with compression. The renal node was demonstrated in no mouse at 10 min, in two mice at 1 h, and in three mice at 3 and 24 h. Thereafter, we performed fluorescence lymph node mapping 3 h after the injection of carboxyl QDs, based on these findings.

Techniques to enhance visualization of lymph nodes

Ventral imaging without shielding demonstrated strong fluorescence from the right popliteal lymph node and weak fluorescence from the iliac lymph node in all five mice at 3 h after the injection of 20 pmol carboxyl QDs (Fig. 4a). The right inguinal lymph node was also observed in one mouse. Intense fluorescence from the right rear foot caused erroneous signals in the right thigh and tail. Shielding the right foot eliminated the signal contamination; however, it did not influence the detection of lymph nodes substantially (Fig. 4b). The delineation of the iliac lymph node was not changed by shielding the right knee (Fig. 4c). Compression of the abdomen improved the visualization of the iliac lymph node (Fig. 4d, e). The signal intensity increased considerably, and visual evaluation indicated reduction in the area of fluorescence when the display scale was adjusted for each image. As a result, the light source could be defined more distinctly. The iliac lymph node/background contrast was 3.64±1.31 (mean ± SD) without compression and 105.53±75.35 with compression. It increased after compression in all mice, and the enhancement ratio was 28.93±22.53.

In the dorsal images with foot shielding, strong fluorescence from the right popliteal and sacral lymph nodes and weak fluorescence from the renal lymph node were observed (Fig. 5a, b). The delineation of the renal node was not changed by hip shielding (Fig. 5c). Compression increased the signal intensity for the renal node mildly; however, the improvement in image quality was not

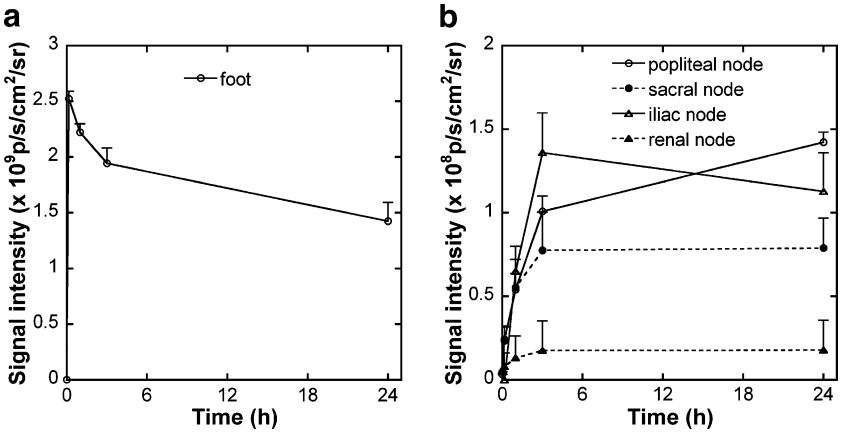

Fig. 3 Time course of fluorescent signal intensities after the injection of carboxyl QDs in the right rear footpad. Average signals in the right rear footpad **a** and lymph nodes **b** are presented. Error bars represent standard errors (n=3)

great (Fig. 5d). Compression increased the renal lymph node/background contrast in all mice (5.15±1.97 without compression, 8.16±3.31 with compression); the enhancement ratio was 1.57±0.25.

Reduction of injection dose

Fluorescence lymph node mapping using 5 pmol carboxyl QDs demonstrated the popliteal and sacral lymph nodes in all three mice. The iliac node was visible in no mouse without compression and clearly visible in all mice with compression (Fig. 6). In one mouse, fluorescence from the renal lymph node was shown indefinitely without compression and definitely with compression. The renal node was not observed in the other mice. Fluorescence lymph node mapping using 1 pmol carboxyl QDs did not demonstrate the renal node in any of the four mice studied. In one mouse, only the right inguinal node was visualized, but not the popliteal, sacral, or iliac node. In the other three mice, the popliteal and sacral nodes were delineated, and the iliac node was visualized only after compression. The inguinal node was also observed in one of the three mice.

Discussion

In this study, we investigated fluorescence lymph node mapping in mice using NIR QDs with special reference to

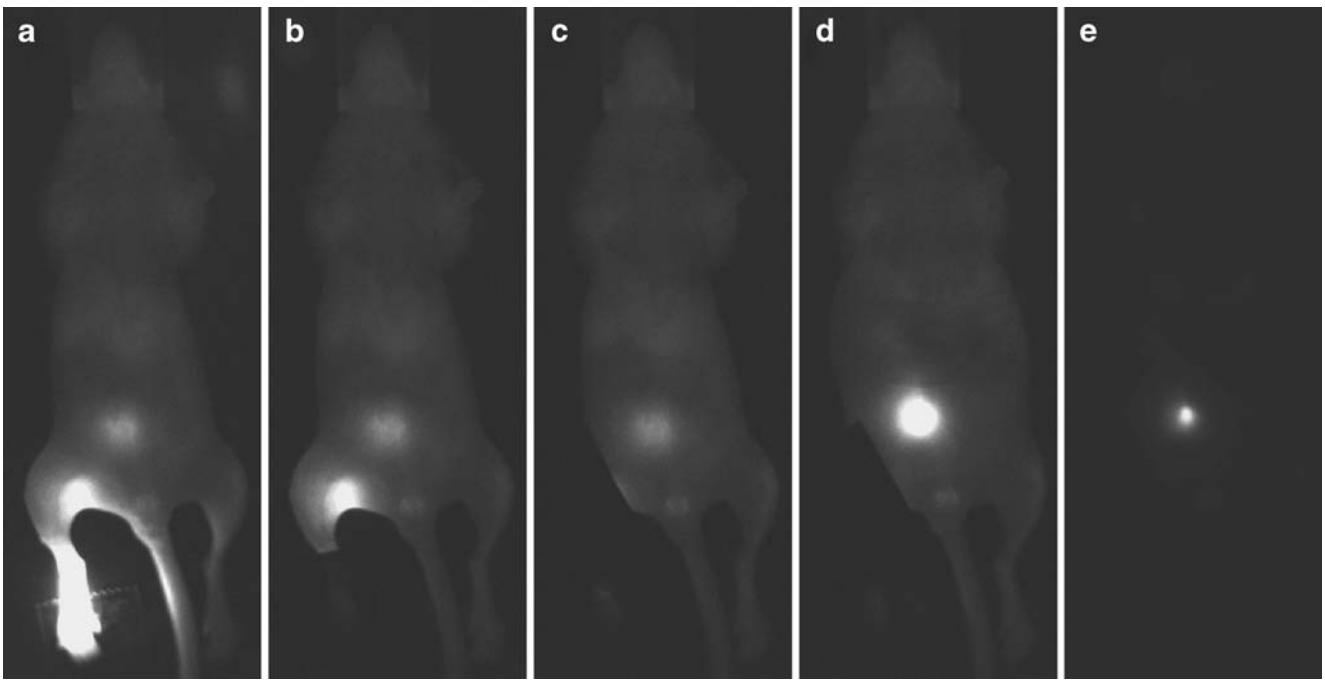

Fig. 4 Ventral images obtained 3 h after the injection of 20 pmol carboxyl QDs. Images were obtained without shielding **a**, with foot shielding **b**, with foot and knee shielding **c**, and with compression **d**, **e**. The same gray scale was used to display panels **a–d** and was adjusted on panel E to indicate the localization of the iliac node signal

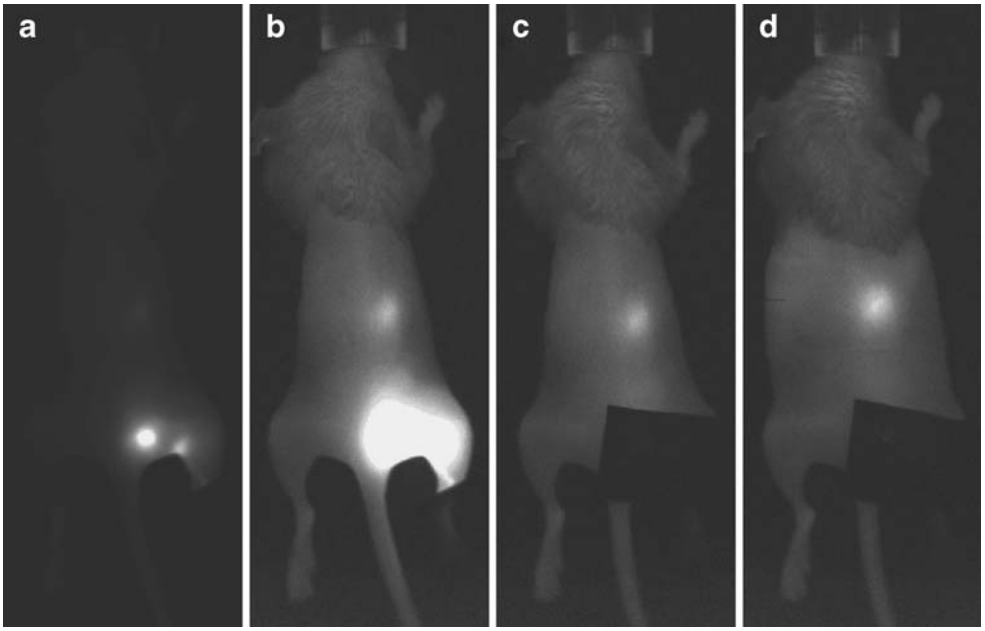

Fig. 5 Dorsal images obtained 3 h after the injection of 20 pmol carboxyl QDs. Images were obtained with foot shielding **a, b**, with foot and hip shielding **c**, and with compression **d**. The same gray scale was used to display panels **b–d** and was adjusted on panel A for better visualization of the popliteal and sacral lymph nodes

the non-invasive visualization of deep abdominal lymph nodes. The most important result of the present study was the successful visualization of the iliac lymph nodes, located deep in the abdomen, with the aid of compression of the abdomen with colorless, transparent tape. Compression moves the intestine and mesentery and decreases the thickness of the tissues overlying the iliac nodes. Shortening the light path reduces the effects of scattering and absorption, allowing the acquisition of clear, high-contrast images. Quantitative analysis of the signal intensity after the injection of 20 pmol QDs demonstrated that compression caused about a 30-fold increase in contrast between the iliac node and background region. As a result of the reduction in scattering, the light source could be localized more distinctly as a small bright spot rather than the large dimly lit area observed before compression. Although the iliac nodes could not be recognized after the injection of 5 pmol QDs without compression, they were visible even using 1 pmol QDs after compression, indicating a large improvement in detection sensitivity, the ability of detecting weak QD accumulation, by the compression technique. This simple technique may be useful not only for fluorescence lymph node mapping, but also for optical imaging in general to visualize deeply located light sources. We did not measure the size of the fluorescent area quantitatively because it was difficult to define the margin

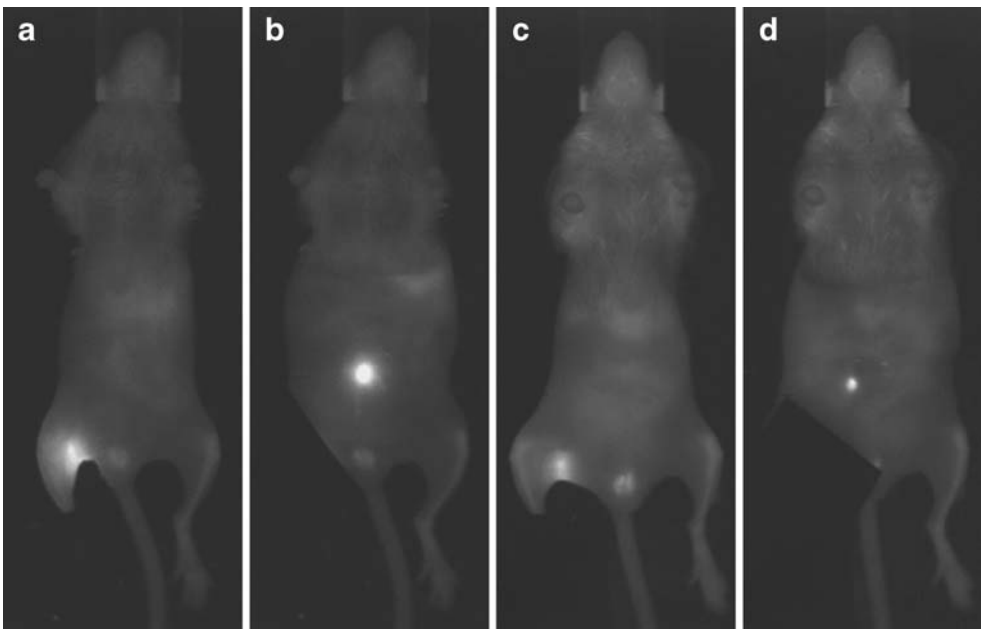

Fig. 6 Ventral images obtained 3 h after the injection of 5 pmol **a**, **b** or 1 pmol **c**, **d** carboxyl QDs. Images were obtained with foot shielding **a**, **c** and with compression **b**, **d**. The same gray scale was used to display images obtained at a given injection dose

of the lymph node signal especially on the images without compression and the measurement appeared to be unreliable. Distinct visualization with compression may facilitate the assessment of the size and allow differentiation between normal and enlarged lymph nodes, which remains to be investigated.

The renal lymph node is located dorsally, behind the caudal vena cava, and was not delineated on ventral images, even with compression. Visualization of the renal node on dorsal images improved after compression; however, the beneficial effect was minimal and the contrast increased by only 57%. The back muscle primarily intervenes between the renal node and body surface in the dorsal projection. The limited effect of compression on visualization of the renal node is likely attributable to the fact that this back muscle is not readily compressed.

Intense light emission may produce erroneous signals in surrounding regions as a result of scattering, which may hinder the detection of the light source of interest. We observed signal contamination from the right rear foot, the injection site, to the right thigh and tail. Such contamination was easily blocked by shielding the injection site with black tape. Although an improvement in lymph node visualization was not apparent in this study, the reduction in signal contamination by shielding may contribute to accurate quantitative evaluations of fluorescence intensity.

Assessment of the time course after QD injection demonstrated definite increases in lymph node signals up to 3 h. Based on these results, we performed lymph node mapping at 3 h after QD injection in all subsequent experiments. The ROI for the iliac node was set on the ventral image with compression, because of the markedly superior image quality provided by compression. Considering the profound signal enhancement by compression, a small variation in the degree of compression may cause substantial changes in quantitative estimates of signal intensity. Thus, standardization of the degree of compression is desirable for quantitative evaluation.

Harrell et al. [10] studied lymphatic drainage in C57BL/6J mice after subcutaneous injection of Evans blue, a conventional dye, into the rear footpad, and demonstrated dye uptake in the popliteal, iliac, renal, and inguinal lymph nodes after sacrifice and dissection. In the present study, using BALB/c mice and carboxyl QDs, the visualization of the inguinal node was uncommon (three of 15 mice), whereas the sacral node was demonstrated in almost all mice (14 of 15 mice). These discrepancies may be attributable to the different mouse strains. The inguinal node alone was demonstrated in one mouse in the present study, suggesting substantial differences in lymphatic drainage patterns, even within a given strain. Alternatively, differences in detection method may have caused the different results regarding the sacral node. In our ex vivo study, the sacral node was covered with tissues and was not readily visible after removal of the skin. Because the fluorescence image showed a bright spot at the site corresponding to the sacral node, we sought the light source there and were able to find the sacral node, using the fluorescence image as a guide. Fluorescence reflectance imaging has the ability to demonstrate light sources covered by other tissues and may offer advantages over the observation of a conventional dye under white light.

QDs are efficiently taken up and retained by the first draining lymph node [11], and have been used for sentinel lymph node mapping in animals [4–7]. We used commercially available carboxyl QDs that had previously been used for lymph node mapping [4, 12, 13]. The negative charge of carboxyl QDs is expected to enhance uptake and retention in the lymph nodes [5]. We observed distant lymph nodes, in addition to the popliteal node located close to the injection site. Such visualization of multiple lymph node regions was demonstrated previously using QDs [6] and was ascribed to the bypass route of the mouse lymphatic system. In mice, communication between afferent and efferent lymphatic vessels allows some lymph to bypass the node [14]. For the assessment of lymphatic drainage from the mouse limb, 8–20 pmol QDs were injected in previous studies [4, 7, 12]. In the present study, the superficial lymph nodes were visualized with 1 pmol, and the iliac nodes were also demonstrated with the aid of the compression technique. Thus, QDs allow lymph node mapping at a low injection dose. Our fluorescence imaging employed a single passband for the detection of emission light. Spectral imaging may allow further improvement in detection sensitivity and reduction of the injection dose [15].

When performing fluorescence imaging in the far-red or NIR region, chlorophyll in the diet generates strong autofluorescence in the gastrointestinal system; for this reason, an alfalfa-free diet is often provided prior to imaging. We demonstrated that a purified diet is more effective than an alfalfa-free diet for the reduction of gastrointestinal autofluorescence in BALB/c nu/nu mice [16]. Because our previous study has suggested that the intake of feces may allow persistent gastrointestinal autofluorescence, we placed a wire rack in the bottom of the cages to prevent feces ingestion and investigated the effect of this arrangement on gastrointestinal autofluorescence. However, successful reduction in gastrointestinal autofluorescence was achieved within 2 days of feeding the purified diet, regardless of the presence or absence of the wire rack, and the intake of the feces was not suggested, even without the wire rack. Differences between wild-type BALB/c mice and BALB/c nu/nu mice may account for this difference in feeding behavior. We fed the mice a purified diet for at least 2 days before fluorescence lymph node mapping and used

the wire rack, although the usefulness of the wire rack was not demonstrated. The successful reduction of gastrointestinal autofluorescence should have contributed to the visualization of abdominal lymph nodes.

Conclusions

Fluorescence lymph node mapping using NIR QDs allowed non-invasive visualization of deep abdominal lymph nodes in addition to superficial lymph nodes in mice. Compression of the abdomen with colorless, transparent tape markedly improved the visualization of the iliac lymph node, as a result of reduced scattering and absorption by overlying tissues. This simple compression technique is expected to enhance the ability of optical imaging to detect deeply located light sources.

Acknowledgements We thank Mr. Haruo Onoda for technical support in histological examinations. We also thank Dr. Lily Wu, University of California, Los Angeles, for helpful discussions. This work was supported in part by a Grant-in-Aid for Scientific Research from the Ministry of Education, Culture, Sports, Science and Technology of Japan.

Conflict of interest No conflict of interest exists in connection with this article.

References

1. Jaiswal JK, Simon SM (2004) Potentials and pitfalls of fluorescent quantum dots for biological imaging. Trends Cell Biol 14(9):497–504
2. Medintz IL, Uyeda HT, Goldman ER, Mattoussi H (2005) Quantum dot bioconjugates for imaging, labelling and sensing. Nat Mater 4(6):435–446
3. Hotz CZ (2005) Applications of quantum dots in biology: an overview. Methods Mol Biol 303:1–17
4. Robe A, Pic E, Lassalle HP, Bezdetnaya L, Guillemin F, Marchal F (2008) Quantum dots in axillary lymph node mapping: biodistribution study in healthy mice. BMC Cancer 8:111
5. Frangioni JV, Kim SW, Ohnishi S, Kim S, Bawendi MG (2007) Sentinel lymph node mapping with type-II quantum dots. Methods Mol Biol 374:147–159
6. Ballou B, Ernst LA, Andreko S, Harper T, Fitzpatrick JA, Waggoner AS, Bruchez MP (2007) Sentinel lymph node imaging using quantum dots in mouse tumor models. Bioconjug Chem 18 (2):389–96
7. Kim S, Lim YT, Soltesz EG, De Grand AM, Lee J, Nakayama A, Parker JA, Mihaljevic T, Laurence RG, Dor DM, Cohn LH, Bawendi MG, Frangioni JV (2004) Near-infrared fluorescent type II quantum dots for sentinel lymph node mapping. Nat Biotechnol 22(1):93–97
8. Weissleder R (2001) A clearer vision for in vivo imaging. Nat Biotechnol 19(4):316–317
9. Ntziachristos V, Bremer C, Weissleder R (2003) Fluorescence imaging with near-infrared light: new technological advances that enable in vivo molecular imaging. Eur Radiol 13(1):195–208
10. Harrell MI, Iritani BM, Ruddell A (2008) Lymph node mapping in the mouse. J Immunol Methods 332(1–2):170–174
11. Tanaka E, Choi HS, Fujii H, Bawendi MG, Frangioni JV (2006) Image-guided oncologic surgery using invisible light: completed pre-clinical development for sentinel lymph node mapping. Ann Surg Oncol 13(12):1671–1681
12. Hama Y, Koyama Y, Urano Y, Choyke PL, Kobayashi H (2007) Simultaneous two-color spectral fluorescence lymphangiography with near infrared quantum dots to map two lymphatic flows from the breast and the upper extremity. Breast Cancer Res Treat 103 (1):23–28
13. Kobayashi H, Hama Y, Koyama Y, Barrett T, Regino CA, Urano Y, Choyke PL (2007) Simultaneous multicolor imaging of five different lymphatic basins using quantum dots. Nano Lett 7 (6):1711–1716
14. Kowala MC, Schoefl GI (1986) The popliteal lymph node of the mouse: internal architecture, vascular distribution and lymphatic supply. J Anat 148:25–46
15. Mansfield JR, Gossage KW, Hoyt CC, Levenson RM (2005) Autofluorescence removal, multiplexing, and automated analysis methods for in-vivo fluorescence imaging. J Biomed Opt 10 (4):41207
16. Inoue Y, Izawa K, Kiryu S, Tojo A, Ohtomo K (2008) Diet and abdominal autofluorescence detected by in vivo fluorescence imaging of living mice. Mol Imaging 7(1):21–7